PM2.5 can Promote the Alzheimer's Disease-like Changes through Microglia Related Mechanism in Mice

Jiaqi Wang
Dalian Medical University
Jie Li
Dalian Medical University https://orcid.org/0000-0003-1365-6132
Jia Wang
Dalian Medical University
Wenping Sun
Dalian Medical University
Qiuyuan Fang
Dalian Medical University
Meiling Meng
Dalian Medical University
Xiao Zhang
Dalian Medical University
Ruxue Jia
Dalian Medical University
Xiaojing Li
Dalian Medical University
Xianzong Meng
RU Nijmegen Donders Institute: Radboud Universiteit Donders Institute for Brain Cognition and Behaviour
Laiyu Song (evasong1984@163.com)
Dalian Medical University

Research

Keywords: PM 2.5, Alzheimer's disease, RNA-Seq, Microglia

Posted Date: October 14th, 2020

DOI: https://doi.org/10.21203/rs.3.rs-90903/v1

$PM_{2.5}$ can Promote the Alzheimer's Disease-like Changes through Microglia Related Mechanism in Mice

Jiaqi Wang[1,#], Jie Li[1,#], Jia Wang[2], Wenping Sun[1], Qiuyuan Fang[1], Meiling Meng[1], Xiao Zhang[1], Ruxue Jia[1], Xiaojing Li[1], Xianzong Meng[3,1], Laiyu Song[1,*]

[1] College of Medical Laboratory, Dalian Medical University, Dalian 116044, Liaoning Province, People's Republic of China.

[2] College of Basic Medical Sciences, Dalian Medical University, Dalian 116044, Liaoning Province, People's Republic of China.

[3] Department of Cognitive Neuroscience, Centre for Neuroscience, Donders Institute for Brain, Cognition and Behaviour, Radboudumc, Nijmegen, The Netherlands.

[#] These authors contribute equally to this work.

*Corresponding author: Laiyu Song (evasong1984@163.com)

Abstract

Background: $PM_{2.5}$, the main particulate air pollutant, poses serious hazard to human health. Alzheimer's disease (AD) is a major neurodegenerative disease characterized by amyloid plaques and neurofibrillary tangles. Recent studies reported that PM could promote AD-like pathologies in human brain. However, the mechanism of $PM_{2.5}$-induced AD-like changes is still unclear and more investigations are needed for further understanding.

Methods: In this study, we established experimental model of long-term $PM_{2.5}$ exposure with young/old wildtype C57BL/6 and APP/PS transgenic mice. Behavior assessments were monitored after four weeks of exposure. The changes of blood cells were detected by Complete Blood Count and splenic macrophages were detected by flow cytometry. Immunohistochemical staining was used to observe the damage of $PM_{2.5}$ on neurons, the deposition of Aβ and the changes of microglia. RNA-seq was used to analyze the whole genome changes of hippocampus after $PM_{2.5}$ exposure. In addition, microglia related genes were analyzed via Real-time PCR.

Results: After mice were exposed to $PM_{2.5}$ for a month, some AD-like behavioral changes, such as learning and memory impairment were detected especially in old and transgenic mice. The histopathological changes, such as β-amyloid (Aβ) deposition, morphological changes of microglia, as well as great impairments of hippocampus neurons but not cortex neurons were observed. The analyze of whole-genome expression in the hippocampus suggested long term $PM_{2.5}$ exposure changed the expression of genes related with AD process (mouse behavior and microglia differentiation). Furthermore, the mRNA level, which related to microglia, of CD86, CD22, IL-1β was upregulated and CD206, TREM2, TGF-β2 was downregulated.

Conclusions: Aged population were more susceptible to long-term $PM_{2.5}$ exposure and $PM_{2.5}$ could promote AD-like phenotype through microglia related mechanism.

Keywords: $PM_{2.5}$; Alzheimer's disease; RNA-Seq; Microglia

1. Introduction

Long-term exposure to $PM_{2.5}$ (the air polluted particles with a diameter less than 2.5 μm) affects the health of billions of people around the world [1], many of whom, especially the people in developing countries, are in very dangerous concentrations of $PM_{2.5}$ [2]. Although $PM_{2.5}$ exposure have been confirmed to play crucial roles in promoting respiratory and cardiovescular diseases [3-7], neurodegenerative diseases, like AD, are attracting more and more researchers' attention [8-11]. Numerous epidemiological and toxicology studies recently demonstrated that $PM_{2.5}$ can cross the Blood Brain Barrier (BBB) and bring about abnormal expression and deposition of Aβ proteins, neuronal damage, chronic inflammation and even AD-like changes [8] in the brain [12-14]. But the clearly function and underlying mechanism are not well illustrated.

AD, characterized by progressive cognitive decline with loss of neurons, is considered to be the most common cause of dementia [15, 16]. With the aging of population becomes more and more serious, the problem of AD, a disorder destroying patients' lives and bringing heavy burdens to the family as well as the society, becomes more and more prominent [16, 17]. The genetic factors and environmental factors are usually recognized as major risk factors for AD [18-20]. All these clues remind the importance of environmental $PM_{2.5}$ exposure in the high incidence of AD at present.

Microglia, which is derived from bone marrow progenitor cell in yolk sac of embryo, are the only immune cells accounts for about 10% of the total cells in central nervous system (CNS) [21]. The crucial character of microglia related neuroinflammation in acute and chronic neurodegenerative diseases, like AD, has been demonstrated by numerous studies. For one thing, microglia could protect neuron cells by engulfing alien substances, clearing cell fragments, Aβ deposition and etc. For another, microglia related inflammatory responses could contribute to the increasing of Aβ deposition, neuron damage and even AD risk [22,

23].

RNA-Seq is a recently developed method for transcriptome profiling using deep sequencing technology [24]. Compared with microarray analysis, this technique is more accurate and more sensitive for characterizing transcriptomes with less confounding effects [25]. Besides providing a precise measurement on gene expression levels, it also owns capability to discover splice junctions, novel transcripts, alternative splice variants and un-annotated genes [26]. In recent years, RNA-Seq has been mostly applied to profile the whole-genome expression of lung tissue or cells after $PM_{2.5}$ exposure. However, applications of RNA-Seq in the effect of $PM_{2.5}$ exposure on CNS have not been reported so far.

In order to clarify the relationship between $PM_{2.5}$ exposure and AD, we established mice model of long-term exposure to $PM_{2.5}$. Young and old wildtype C57BL/6 mice and APP/PS transgenic mice were used to explore the effects of $PM_{2.5}$ on different groups. We found that $PM_{2.5}$ exposure could induce AD-like changes and had a significant effect on the hippocampus of mice, especially in the aged group. RNA-Seq was performed on the hippocampus of the aged group to screen out possible mechanisms and targets. Microglia-related changes were detected and reexamined by Real-time PCR and immunohistochemical staining. All data proved that aged population were more susceptible to long-term $PM_{2.5}$ exposure and $PM_{2.5}$ might promote AD-like phenotype through microglia related mechanism.

2. Materials and methods

2.1 Animals

Male C57BL/6 mice were purchased from the Dalian Medical University Laboratory Animal Centre, APPswe/PS1dE9 C57BL/6 J double-transgenic (APP/PS1) male mice on C57BL/6 background were purchased from Nanjing Medical University Animal Model Institute. All animals were housed 4-5 per cage at 22±2°C with a 12h light/dark cycle. Animal experiments performed in compliance with the National Institutes of Health guidelines for the use of laboratory animals. The ethical standards of the experiments were in accordance with the guidelines provided by the Committee for the Purpose of Control and Supervision of Experiments on Animals. The experiments were designed to include control groups for all experiments as well as randomized procedures and to apply blinded analysis whenever possible.

After a 7-day acclimatization period to the new environment, young (3.5 months old), old (12 months old) and APP/PS (3.5 months old) mice were weighting 25-35g and then divided into: Con-young group: Saline only (n = 6), $PM_{2.5}$-young group: $PM_{2.5}$+Saline (n = 6); Con-old group: Saline only (n = 6), $PM_{2.5}$-old group: Saline+$PM_{2.5}$ (n = 6); Con-APP/PS group: Saline only (n = 6), $PM_{2.5}$-APP/PS group: Saline+$PM_{2.5}$ (n = 6) randomly by weight. After the division of each group, mice were either treated with the $PM_{2.5}$ suspension (100μg/20ul) or with filtered sterile saline (20ul, n=6) by intra-tracheal instillation once every other day for 4 weeks.

2.2 $PM_{2.5}$ collection and preparation

The $PM_{2.5}$ samples were prepared according to previously published methods [27]. Briefly, $PM_{2.5}$ was collected on ultra-fine quartz fiber filters using a $PM_{2.5}$ air sampler, four-stage multinozzle cascade impactor (MCI) (Tokyo Dylec Corp., Tokyo, 79 Japan), from Dalian (Liaoning, China). The filters adhering $PM_{2.5}$ were cut into small pieces and immersed

126 in sterile distilled water, followed by ultrasonic, vacuum-freeze drying, weighed and stored at
127 −20°C until use. The particles were diluted with sterile saline into $PM_{2.5}$ suspension with a
128 concentration of 10mg/mL. The $PM_{2.5}$ suspension was always sonicated and vortexed before
129 use.

130 **2.3 Behavioral Testing**

131 **2.3.1 Elevated Plus Maze Test (EPM)**

132 EPM was used to evaluate the anxiety-like state of animals, because it could reflect the
133 conflicting behaviors caused by the characteristics of exploring new and different
134 environments and the aversion to open spaces and heights [28]. The maze is made of white
135 acrylic glass plate, including two open arms (30×5 cm) and two enclosed arms (30×5×15 cm)
136 [29]. The four arms radiate outward at a 90-degree angle and a central platform (5×5 cm) was
137 used to connect the arms such that the same kind of arms could be opposite to each other. The
138 maze was placed at 55 cm above the ground.

139 At the beginning of the experiment, each animal was placed into the central platform
140 facing the open arms and allowed to explore the maze freely for 5 minutes. The arms were
141 cleaned with 75% ethanol after each trial in this test. All mice's performances were recorded
142 by video and the total amount of time spent in open arms and the closed arms was calculated
143 [30]. The reduction of the exploration time in open arms was regarded as increased anxiety.

144 2.3.2 Sucrose Preference Test (SPT)

145 SPT is widely accepted to evaluate the depressive-like behavior in mouse [31]. The
146 experiment was conducted as described previously [32] Briefly, animals were given two
147 bottles of 1% sucrose solution in the first training day. In the second training day, animals
148 were served with one bottle of 1% sucrose solution and one bottle of sterile water. After two
149 days of training, the formal experiment was conducted. We gave the animal two bottles of
150 liquid in each animal's cage to choose, one bottle of sterile water and one bottle of 1%

sucrose solution. And the bottle positions were switched after 12 h to prevent a position preference. Each bottle was weighed and the consumption was calculated 24 hours later (grams converted to ml). The sucrose preference was calculated by the following formula: Sucrose preference (%) = (sucrose intake(ml)/total fluid intake(ml)) × 100%. The calculation was conducted according to previous work [33-35].

2.3.3 Morris Water Maze Test (MWM)

MWM, an important cognitive test for neurodegenerative diseases like AD, was performed to test spatial learning and memory of animals[36]. The maze in this work is a circular tank (120 cm in diameter and 50 cm in height), filled with water to 30 cm height (22±1°C). The maze was divided averagely into four equal quadrants and a hidden circular platform (10 cm in diameter) was submerged 1 cm below the water surface in the center of the third quadrant. Entry points, which were systematically used throughout the experiment, were in other three quadrants and spaced equally around the edge of the tank. Briefly, the animals were trained for 90 seconds repeatedly to find the platform using visual information around and time taken (escape latency) to find the hidden platform was recorded as the learning (acquisition) process [37]. Mice who can not find the platform within 90 seconds were guided to the platform and the escape latency of it was recorded as 90 seconds. The animal motion was recorded and sent to the computer by a digital camera mounted above the center of water maze.

To assess the spatial memory retention of these mice, the spatial probe test was performed 24 hours after the final acquisition session of the navigation test above. In spatial probe test, the platform was taken away and mice were allowed to explore the maze for 60 seconds. Record all the performance and figure out the number of times they crossed the original platform position and the percent of time and distance in the third quadrant.

2.3.4 Y-Maze

Y-Maze was used to assess spatial learning and memory in mice. The maze consists of three arms (47×46×16 cm) and each arm of this Y-maze was positioned at 120° equally. In the spontaneous alternation test, each mouse was placed at the end of the same arm, the mouse was allowed to freely explore the maze for 8 min. As previously described, we recorded the whole body entries (4 paws inside an arm) of mice into all arms and counted spontaneous alternation when an animal entered three different arms consecutively [38]. The percentage of spontaneous alternation was calculated by the following formula: [(number of alternations)/(total number of arm entries − 2)] × 100% [39].

2.4 Complete Blood Count (CBC)

After the behavioral experiment, blood was collected via retro-orbital, 200µl venous blood was taken into a vacuum vessel containing ethylene diamine tetra acetic acid (EDTA) anticoagulant. All measurements were performed on the hematologic analyzer Sysmex XN-1000.

2.5 Cell isolation and Flow cytometry

After the excision of spleen, place it in a 200-mesh cell sieve and grind it thoroughly and mechanically dissociated in cold phosphate buffer saline (PBS). After lysis of red blood cell (RBC), spleen cells were washed and re-suspended in PBS. Fluorescence staining was performed using CD11b antibodies purchased from Abcam. Briefly, the cells from spleen were re-suspended in PBS and Fc receptors were blocked with purified anti-mouse CD16/32 for 30 min at 4°C. Single cell suspension of spleen were incubated with anti-mouse CD11b-APC (clone: M1/70 eBioscience) for 20 min at 4°C in the dark. Following incubation, washing with PBS were performed. After washing, the cells were resuspended in PBS, and analyzed by flow cytometry on a ACEA NovoCyteTM instrument with Novoexpress software. According to the negative control, the position of CD11b+ cells was analyzed. Results were expressed as the percentage of CD11b+ cells (the cells in the right gate/shoulder)

2.6 Immunohistochemistry

The hippocampus was cut coronally on a frozen sliding microtome (20μm/tablet). These 20μm coronal sections were obtained with a Leica CM1850 cryostat. Slices were collected free floating in PBS and processed for immunohistochemistry. Each brain (located approximately 3.10-1.68 mm from interaural) was cut into about 60-70 slices at the same level. All immunohistochemical and cell counting procedures have been published previously [40-43]

In brief, after blocking and washing, brain slices were incubated with diluted primary antibody at 4°C overnight in PBS with 0.25% Triton X-100 (PBST). The next day, the slices were rewarmed for 1 h at room temperature, and then incubated with corresponding secondary antibody for 30 min and a streptavidin-biotin system for 30min (KIT-9720; Ultrasensitive TMS-P, Maixin Biotech, Inc., Fuzhou, China). Finally, stained the brain slices with the diaminobenzidine tetrahydrochloride (DAB) method.

Ionized calcium binding adapter molecule 1 (Iba1) is a microglia/macrophage-specific calcium-binding protein [44]. Microtubule-associated protein 2 (MAP-2) is usually used as a specific marker for neurons[45]. Amyloid-betape pticle (Aβ1-42) is regarded as the main and special pathological feature of AD[62]. The following primary antibodies were therefore used for marker detection: anti-IBA-1 antibody (019-19741; Wako Pure Chemical Industries, Ltd, Japan) (1:2000), anti-MAP-2antibody (GTX133109;Gene Tex,USA) (1:800), anti-Aβ1-42 antibody (GTX134510-S; Gene Tex, USA) (1:1000).

An Olympus IX-71 microscope with a three-axis motorized stage, video camera and Image J (National Institutes of Health, Bethesda, MD, USA) was used for image analysis. Three sections of each mouse (one out of six slices distributed from hippocampus (3.10-1.68 mm from Interaural) for staining Nissl, MAP2, IBA-1, Aβ1-42 respectively) were taken for counting, and matched for level as closely as possible from animal to animal. To get the same

amount of light, the intensity of light was adjusted for unstained control areas in the same section. The collected Iba-1 and Aβ1-42 staining images were transformed into integrated optical density (IOD) images by use of a standard transformation curve by Image-Pro Plus 6.0 software.

2.7 Nissl Staining

Hippocampal and cortex neurons were visualized by Nissl staining. The brain slices were stained with thionine at 37°C for 20 min, the slices were subsequently dehydrated with 70, 75, 90, 95, and 100% alcohol, washed in xylene. Image were imaged by the bright field microscopy, the number of surviving neurons in the CA1 of the hippocampus and cortex were manually circled and counted within a unbiased counting fields (100μm×100μm) per group. Each slices was counted in three segments, and the average number was the neuronal density (ND).

2.8 Extraction of total RNAs

Fresh tissue was collected, flash frozen and stored at −80 °C. Hippocampi dissected out in sterile saline after brains thawed. Total RNAs of mice Hippocampi were extracted by using TRIZOL reagent (Invitrogen Life Technologies, USA) following the manufacture's protocol. The concentration and purity of the RNAs were checked by Nanodrop 2000 (Thermo Fisher Scientific, USA). For RNA sequencing, the RNA integrity was assessed by analyzing standard denaturing agarose gel electrophoresis and Agilent 2100 was used to determine RNA integrity number (RIN) value.

2.9 Library construction, RNA sequencing and data analysis

Firstly, rRNAs in samples from control and $PM_{2.5}$ groups were removed. Then, the libraries for next generation sequencing were prepared using the TruseqTM RNA sample prep Kit for Illumina (Illumina, USA) according to the manufacturer's instructions. After enrichment and purification, the libraries were processed for sequencing by Shanghai

Origingene Bio-pharm Technology Co. Ltd (Shanghai, China) according to an available protocol. After quality control of the original data, the high-quality sequencing data is compared with the designated reference genome. The theexpression values is calculated by the StringTie tool, and tDESeq algorithm was applied to filter the differentially expressed genes. Gene ontology (GO) and Kyoto encyclopedia of genes and genomes (KEGG) analysis was performed to facilitate exploring functions of differentially expressed genes and pathways involved.

2.10 Real-time PCR analysis

Real-time PCR was performed using the SYBR Green ER qPCR Super Mix Universal kit with specific primers listed below. The universal two-step reverse transcriptase PCR cycling conditions used were as follows: 95 °C for 30s, 95 °C for 5s, followed by 40 cycles of 60 °C for 30 s. The primer sequences used are listed in Table 1. All data were calculated using the $2^{-\Delta\Delta}$Ct method.

Table 1. Primers sequence for Real-time PCR analysis

Gene Target	Forward Primer Sequence (5'-3')	Reverse Primer Sequence (5'-3')
CD86	GACCGTTGTGTGTGTTCTGG	GATGAGCAGCATCACAAGGA
CD206	TTCGGTGGACTGTGGACGAGCA	ATAAGCCACCTGCCACTCCGGT
TREM2	CACTCTGAAGAACCTCCAAGC	ATTCCTGGAGGTGCTGTGTT
CD22	CCACTCCTCAGGCCAGAAACT	TGCCGATGGTCTCTGGACTG
TGF-β2	GTGAATGGCTCTCCTTCGAC	CCTCGAGCTCTTCGCTTTTA
IL-1β	CCAGCAGGTTATCATCATCATCC	CTCGCAGCAGCACATCAAC
GAPDH	AAATGGTGAAGGTCGGTGTGAAC	CAACAATCTCCACTTTGCCACTG

2.11 Statistical Analysis

Statistical analyses were carried out using SPSS Statistics version 21.0 (SPSS Inc, Chicago, IL). The data are presented as the mean±standard error of the mean (S.E.M.). Briefly as described previously [43], the data between control and $PM_{2.5}$ model group were analysed using independent Student t-test. Multiple groups were analyzed by one-way ANOVA followed by a Fisher's least significant difference (LSD) post-hoc correction. The

figures were made by GraphPad Prism version 7.0 (GraphPad Software, San Diego, CA, USA). Statistical significance was assumed at *p<0.05, ** p<0.01, *** p<0.001. vs Control group. $^{\#}$P<0.05, $^{\#\#}$P<0.01, $^{\#\#\#}$P<0.001 vs Young groups after PM2.5 exposure. P values lower than 0.05 were considered as statistically significant.

3. Results

3.1 The systemic inflammation after $PM_{2.5}$ exposure

The investigations of PM2.5 exposure usually focused on inflammatory responses related with respiratory and circulatory system. Systemic inflammation was also suggested to contribute to the neurodegenerative diseases [46]. Therefore, we first examined the systemic inflammation after $PM_{2.5}$ exposure. The results of peripheral hemogram showed an increase of total leukocyte counts per liter after long term $PM_{2.5}$ exposure especially in APP/PS transgenic AD model. $PM_{2.5}$ aspiration also increased the platelets (PLT) level in peripheral blood. RBC counts per liter was almost not changed at all (Table.2)

Table 2. Complete Blood Count (CBC) results of young, old and APP/PS mice.

	Con-young	$PM_{2.5}$-young	Con-old	$PM_{2.5}$-old	Con-APP/PS	$PM_{2.5}$-APP/PS
Leukocyte(10^9/L)	11.96 ± 1.433	12.82 ± 1.001	11.63 ± 1.557	11.68 ± 0.661	5.254± 0.340	8.623± 0.677**
RBC (10^{12}/L)	10.23±0.095	10.47± 0.177	9.536±0.168	9.977 ± 0.146	9.882± 0.158	9.878 ± 0.187
PLT (10^9/L)	800± 61.29	1015± 53.18*	1071± 116.3	1246 ± 13.8	824± 5.333	1134 ± 86.31*

* $p < 0.05$ for $PM_{2.5}$-young mice vs. Con-young mice; $PM_{2.5}$-APP/PS mice vs. Con-APP/PS mice

** $p < 0.01$ for $PM_{2.5}$-APP/PS mice vs. Con-APP/PS mice

Considering the majority (~90%) of CD11b+ splenocytes were monocytes, we then re-examined the systemic inflammatory response in the biggest peripheral immune organ by flowcytometry. As shown in Figure.1, $PM_{2.5}$ exposure increased the percentage of CD11b+ splenocytes in the young, old and the APP/PS transgenic AD groups significantly, and the increasing rate were about 23.5%-27% (Figure.1).

3.2 Effects of long term $PM_{2.5}$ exposure on spatial learning and memory

To examine the effect of $PM_{2.5}$ exposure on spatial learning and memory of mice, Morris

water maze and Y maze were used in this experiment. In MWM, $PM_{2.5}$ exposure did not change the swimming speed of mice in the learning phase (Figure.2C). The escape latency, time to reach to the hidden platform, was longer after $PM_{2.5}$ exposure (Figure.2A) especially at the fifth day of training (Figure.2B). In the probe trial, the time percent spent in the platform quadrant decreased after $PM_{2.5}$ exposure (Figure.2D). The percent of the swimming distance in the platform quadrant and the number of times crossings the target quadrant were also decreased significantly after $PM_{2.5}$ exposure (Figure.2E, F). The results of Y-maze showed that the percentage of spontaneous alternation of mice in $PM_{2.5}$ treatment groups were significantly lower than those of the corresponding control groups (Figure.2G) on the condition that there was no significant difference in the total number of arm entries between the $PM_{2.5}$ treatment groups and the corresponding control groups (Figure.2H). All the results above suggested that the spatial learning and memory of mice was impaired after $PM_{2.5}$ exposure in this work.

3.3 Effects of long term $PM_{2.5}$ exposure on the affective behaviors

After 4 weeks of $PM_{2.5}$ suspension/saline treatment, the animals in each group were weighed. $PM_{2.5}$ exposure did not change the body weight significantly (Figure.3A). Then, EPM (for anxiety-like behavior) and SPT (for depressive-like behavior) were used to measure the affective behaviors of mice. In EPM test, $PM_{2.5}$ caused a reduction of the time spent in the open arms. The reduction was most significantly in the APP/PS transgenic AD group (Figure.3B). This time decreasing induced by $PM_{2.5}$ was not significant in old group (Figure.3B). But the sucrose preference decreased significantly only in the old group after $PM_{2.5}$ exposure (Figure.3C). All the results above reminded us that the $PM_{2.5}$ might have a greater impact on the affective behaviors of old and the AD population.

3.4 Learning and memory impairment may be caused by hippocampus neuron damage after $PM_{2.5}$ exposure

Considering the behavioral changes of mice after $PM_{2.5}$ exposure, we then examined the pathological changes of hippocampus and cortex by Nissl staining and immunohistochemistry. The results of Nissl staining of hippocampus CA1 area showed that the neurons in young control groups exhibited a normal morphology and were neatly arranged (Figure.4A). The pyramidal neurons in the hippocampus CA1 area of animals in the old control group and the APP/PS transgenic AD control group were slightly disordered, with unclear cell structure and deep staining (Figure.4A).

Compared with the corresponding control groups, the pyramidal cell layers in the hippocampus CA1 area in each $PM_{2.5}$ treatment group were thinner, the neuron arrangements were disordered and loose, with unclear unity and arrangement, and a large number of neuron structures disappeared (Figure.4A). As shown in Figure 4, cortical neurons of animals in control groups had clear cell structure, full nuclei and rich Nissl bodies in their cytoplasm. Compared with the corresponding control groups, the cortical neurons of each $PM_{2.5}$ treatment group showed slightly fuzzy cell structure, and slightly decreased cell density of positive cells with Nissl staining, but there is no statistical difference (Figure.4B).

MAP2 is a microtubule-binding protein 2 specifically expressed on neurons. As shown in Figure 5, there was no significant difference in the number of MAP2 positive cells between young, old and APP/PS transgenic AD control groups. The arrangement of neurons of hippocampus were dense and orderly, with regular morphology and clear staining. In the young $PM_{2.5}$ group, the neurons of hippocampus were not neatly arranged with unclear staining and lower expression of MAP2 (Figure.5). In the old $PM_{2.5}$ group, neurons of hippocampus were irregularly arranged, with large areas without staining, and the expression of MAP2 was seriously absent (Figure.5). In APP/PS transgenic AD group, neurons of hippocampus were disordered and loose in cell arrangement, and there were several small areas without staining around the cells after $PM_{2.5}$ exposure (Figure.5). $PM_{2.5}$ exposure did

not influence the cortical neurons in different groups (data was not shown). All these results above suggested that the hippocampus neurons were more vulnerable to $PM_{2.5}$ exposure. The hippocampus neurons injury might be responsible for the learning and memory impairment in this model.

3.5 Alzheimer's Disease-liked pathological changes after $PM_{2.5}$ exposure

Stage-specific accumulation of Aβ is the pathological hallmarks of AD. As shown in Figure 6, there were no expression of Aβ1-42 in the hippocampus CA1 region of young control or $PM_{2.5}$ treated mice, but a small amount of Aβ1-42 aggregates scattered in the hippocampus CA1 of the old control group and the APP/PS transgenic AD group (Figure.6). Compared with that of corresponding control groups, the Aβ1-42 in hippocampal CA1 of old $PM_{2.5}$ group and APP/PS transgenic $PM_{2.5}$ group were significantly increased (Figure.6). Mice developed pathological characteristics which similar to Alzheimer's disease.

3.6 Changes in transcriptomics of hippocampus tissue after $PM_{2.5}$ exposure

To explain the reasons for above results, we performed RNA-Seq on hippocampus. Analyzing the results showed that $PM_{2.5}$ has a highly significant effect on gene expression in hippocampus of aged mice. In total, 479 genes were identified as differentially expressed genes ($p<0.05$) (Figure.7), compared with control group, 125 mRNAs were upregulated and 354 mRNAs were downregulated in $PM_{2.5}$ group (Figure.7).

As shown in Figure.8, in ddition to the conventional enriched extracellular matrix related genes, Gene Ontology (GO) analysis suggested the adhesion and migration related genes account for a large part of the top 45 classification. Kyoto Encyclopedia of Genes and Genomes (KEGG) analysis suggested that the microglial function related genes expression, like phagosome, inflammatory diseases, immune responses were most enriched among the differentially expressed genes (Figure.9). Analysis of the results of RNA-Seq showed that during this AD-like phenotype process, obvious changes have occurred in the differentiation

markers of microglia, like CD206 (Figure.7).

3.7 Detection of microglia related changes after $PM_{2.5}$ exposure by Real-time PCR and Immunohistochemical staining

To validate the RNA-Seq results in this study, we confirmed the RNA-Seq data using Real-time PCR. As shown in Figure 10, after $PM_{2.5}$ exposure (all the young group, old group and APP/ PS transgenic group), CD86 was upregulated (Figure.10A) and CD206 was downregulated (Figure.10B). Further, genes related to phagocytosis,TREM2 was downregulated (Figure.10C) and CD22 was upregulated (Figure.10D), inflammatory related gene IL-1β was upregulated (Figure.10E), and an anti-inflammatory gene TGF-β2 was downregulated (Figure.10F). This change was more obvious in the old and the APP/PS transgenic groups.

Then, we examined the level of IBA-1, a calcium ion binding molecule specifically expressed on microglia, to reflect the morphology and number of microglia in hippocampus after $PM_{2.5}$ exposure. The results of IBA-1 immunohistochemistry show that, compared with the young $PM_{2.5}$ group, the number of microglia in both the old and the APP/PS transgenic $PM_{2.5}$ groups increased to different degrees, and the increase of microglia in the old mice is the most significant (Figure.10H). The number and morphology of microglia in the hippocampal area of the mice treated with $PM_{2.5}$ significantly changed, and the number of cells, size of cell body and branch complexity all increased, showing an obvious activation state (Figure.10G). All the results indicated that $PM_{2.5}$ may promote the Alzheimer's disease development through microglia dependent mechanism.

4. Discussion

The results of this study suggested that long-term exposure to $PM_{2.5}$ could promote the progression of AD, accompanied by damage to hippocampal neurons and deposition of Aβ and microglia may play crucial roles in this model. The results also reminded that the hippocampus of the elderly and AD patients were more susceptible to $PM_{2.5}$. To our knowledge, our study was the first animal experiment to demonstrate the relationship between $PM_{2.5}$ and AD with long-term exposure by using RNA-seq. We investigated possible mechanisms and provided potential targets for further research and treatment of AD.

Numerous studies and our previous researches have shown that $PM_{2.5}$ can enter the lungs through breathing, causing oxidative damage and inflammatory response to the lung and heart [47-49]. Only a few studies have focused on the effects of $PM_{2.5}$ on the brain. In 2002, Oberdörster et al first reported that the target of PM in the brain should be concerned [50]. Generally, the process of PM affecting brain is considered to occur through two pathways. On the one hand, particles may get access to the brain through nasal olfactory pathway [51-54]. On the other hand, PM could trigger the release of inflammatory mediators from primary entry organs or secondary deposition sites [10, 55], which may cause or alter the brain's susceptibility to neuroinflammation and neurodegeneration [55]. In recent years, population-based studies from Mexico City have reported that air pollutants including PM might promote AD-like pathologies [56]. Almost all studies in this field just focus on clinical data analysis or population sample statistics, but few researches concern about the underlying mechanism of AD-like changes induced by long term $PM_{2.5}$ exposure. Considering the different incidence of AD in different age groups, we used mice of different ages and gene backgrounds to explore the relationship between long-term $PM_{2.5}$ exposure and AD. We also wanted to figure out the underlying mechanism and potential target of $PM_{2.5}$ in the process of AD in this work. Firstly, after exposed to $PM_{2.5}$ for one month, the increased level of

leukocytes and PLT in peripheral hemogram suggested a successful $PM_{2.5}$ exposure and systemic inflammation. Meanwhile, the increased level of monocyte in the spleen suggested that monocytes may play crucial role in this model.

AD is a disease characterized by learning and memory disorders, and the incidence rate of AD is high in the elderly [15]. We then observed the effects of $PM_{2.5}$ exposure on learning and memory behavior of mice through the MWM and Y-maze experiments. We used different type of mice (young, old and APP/PS transgenic) to explored the relationship between AD and long term $PM_{2.5}$ exposure separately. Our results suggested that $PM_{2.5}$ exposure impaired spatial learning and memory significantly[26], especially for old and APP/PS transgenic mice. $PM_{2.5}$ exposure also influenced the affective behaviors especially for old and APP/PS transgenic mice. But this effect on affective behaviors was not too strong, which consistent with the results of epidemiological investigations that some Alzheimer's patients suffered from depression during the memory deterioration stage [56, 57].

The important roles of hippocampus and cortical in learning and memory have been demonstrated by a lot of investigations [58-60], we therefore examined the morphological of neurons in these areas. The neuron damage in hippocampus is a typical pathological characteristic of AD. Previous investigation demonstrated that the maturation of hippocampal neurons was inhibited and the complexity of dendrites was significantly reduced in SD rats after exposed to ammonium sulfate for a long time [61]. After $PM_{2.5}$ exposure, the results of Nissl staining and MAP2 in cortex showed that the damage degree of cortical neurons were not as obvious as that of hippocampus in mice, which suggested the hippocampus might be more vulnerable in this model.

The disposition of Aβ 1-42 in brain is the main and special pathological feature of AD [62]. We then examined the Aβ amyloid in hippocampus by immunohistochemical stain to explore the relation between long term $PM_{2.5}$ exposure and AD. No Aβ could be found in the

hippocampus of young $PM_{2.5}$ mice, but the Aβ amyloid deposition increased significantly in the hippocampal CA1 region of old and APP/PS transgenic AD mice. The trend of these immunohistochemical results was consistent with our previous behavioral results. All these suggested that long-term inhalation of $PM_{2.5}$ might induce AD, and the old population and people with AD family genetic disorders are more susceptible.

Considering the different effect of $PM_{2.5}$ among different groups and significant impact on hippocampal tissues, we chose the hippocampal tissues of old mice for RNA-Seq analysis to further explore the underlying epigenetics mechanisms in a systematic perspective. From the transcriptome analysis, 125 increased genes and 354 decreased genes were detected after long term $PM_{2.5}$ exposure. KEGG analysis showed 39 pathways participated the disorders induced by $PM_{2.5}$, belonging to Environmental Information Processing, Human Diseases, Organismal Systems, Cellular Processes. The enrichment analysis of these genes also strongly supported the linkage between long term $PM_{2.5}$ exposure and the function of microglia, like phagocytosis, immune responses and systemic inflammation, most of which reminded the participation of microglia in this model. Microglia is the innate immune cells of CNS. Proliferation and activation of microglia in the brain, concentrated around amyloid plaques, is a prominent feature of AD [63]. The occurrence and development of AD has also been proved to be related to microglia [22, 23]. In order to verify the results of RNA-Seq and our speculation in this model, we re-examined the expression of microglia-related genes in the hippocampal tissue by Real-time PCR. As expected, the tendency of these results was consistent with that of RNA-Seq, especially in the elderly. The shifted markers of M1/M2, the increased phagocytosis-related genes and the changed inflammatory factors suggested the crucial role of microglia after long term $PM_{2.5}$ exposure especially in old and AD groups. We also confirmed the interaction between long term $PM_{2.5}$ exposure and microglia in AD like process by morphology examination. All the results above suggested that after long-term

493 $PM_{2.5}$ exposure, microglia related immune and inflammatory responses may play crucial roles
494 in the development of learning and memory disorders and AD-like changes.
495
496 **Conclusions**
497 In summary, the presented results gave the first positive connection between long-term
498 $PM_{2.5}$ exposure and AD development based on RNA-seq analysis of mouse model. Long-
499 term exposure to $PM_{2.5}$ can induce/promote AD, especially in the elderly and AD population.
500 The damage of neurons and Aβ1-42 deposition became more serious in mouse hippocampus
501 after $PM_{2.5}$ exposure. Furthermore, microglia played a vital role in our model, and a microglia
502 dependent immune and inflammatory mechanism might be involved in $PM_{2.5}$ induced AD-
503 like changes and promote Alzheimer's disease progression in CNS. Interfering with this
504 pathway may have therapeutic and preventive value for AD in future.
505
506 **Abbreviations**
507 AD: Alzheimer's disease; BBB: Blood Brain Barrier; CNS: Central nervous system; MCI:
508 Multinozzle cascade impactor; EPM: Elevated Plus Maze Test; SPT: Sucrose Preference Test; MWM:
509 Morris Water Maze Test; CBC: Complete Blood Count; PBS: Phosphate buffer saline; RBC: Red
510 blood cell; DAB: Diaminobenzidine tetrahydrochloride; Iba1: Ionized calcium binding adapter
511 molecule 1; MAP-2: Microtubule-associated protein 2; Aβ1-42: Amyloid-betape pticle; IOD:
512 Integrated optical density; ND: Neuronal Density; RIN: RNA integrity number; GO: Gene ontology;
513 KEGG: Kyoto encyclopedia of genes and genomes; PLT: Platelets;
514
515 **Acknowledgments**
516 We would like to thank Chunqing Liu in particular. She participated in experimental design, animal
517 experiments and manuscript writing.
518

Authors' contributions

Laiyu Song and Jiaqi Wang: overall organizing of the experiments; Jiaqi Wang, Jie Li, Qiuyuan Fang， Meiling Meng, Xianzong Meng, Xiaojing Li and Xiao Zhang: performed the experiments; Xianzong Meng, Jiaqi Wang, Jie Li and Laiyu Song wrote the paper; Wenping Sun, Jia Wang and Laiyu Song: designed the experiments. All authors have read and approved the final manuscript. The final manuscript was approved by all authors.

Funding

This study was supported by the National Natural Science Foundation of China grants (81502776) and the Seedling project of Liaoning Province (Grant No. 354 LZ2019065); the Special Grants for Scientific and Technological Innovation of Dalian (2017RQ123); the Special Grants of Liaoyang thrombus hospital.

Availability of data and materials

The datasets used and/or analyzed during the current study are available from the corresponding author on reasonable request.

Ethics approval and consent to participate

All animal protocols were approved by the Animal Care and Use Committee of Dalian Medical University in Liaoning.

Consent for publication

Not applicable

Competing interests

The authors declare that they have no competing interests.

Author details

[1]College of Medical Laboratory, Dalian Medical University, Dalian 116044, Liaoning Province, People's Republic of China. [2]College of Basic Medical Sciences, Dalian Medical University, Dalian 116044, Liaoning Province, People's Republic of China. [3]Department of Cognitive Neuroscience, Centre for Neuroscience, Donders Institute for Brain, Cognition and Behaviour, Radboudumc, Nijmegen, The Netherlands.

References

1. Ren M, Fang X, Li M, Sun S, Pei L, Xu Q, Ye X, Cao Y: **Concentration-Response Relationship between PM2.5 and Daily Respiratory Deaths in China: A Systematic Review and Metaregression Analysis of Time-Series Studies.** *Biomed Res Int* 2017, **2017:**5806185.
2. Liu X, Frey HC: **Modeling Of In-Vehicle Human Exposure to Ambient Fine Particulate Matter.** *Atmos Environ (1994)* 2011, **45:**4745-4752.
3. Guo Y, Mishra A, Howland E, Zhao C, Shukla D, Weng T, Liu L: **Platelet-derived Wnt antagonist Dickkopf-1 is implicated in ICAM-1/VCAM-1-mediated neutrophilic acute lung inflammation.** *Blood* 2015, **126:**2220-2229.
4. Xu H, Jiao X, Wu Y, Li S, Cao L, Dong L: **Exosomes derived from PM2.5treated lung cancer cells promote the growth of lung cancer via the Wnt3a/betacatenin pathway.** *Oncol Rep* 2019, **41:**1180-1188.
5. Pratali L, Marinoni A, Cogo A, Ujka K, Gilardoni S, Bernardi E, Bonasoni P, Bruno RM, Bastiani L, Vuillermoz E, et al: **Indoor air pollution exposure effects on lung and cardiovascular health in the High Himalayas, Nepal: An observational study.** *Eur J Intern Med* 2019, **61:**81-87.
6. Pun VC, Kazemiparkouhi F, Manjourides J, Suh HH: **Long-Term PM2.5 Exposure and Respiratory, Cancer, and Cardiovascular Mortality in Older US Adults.** *Am J Epidemiol* 2017, **186:**961-969.
7. Qi Z, Song Y, Ding Q, Liao X, Li R, Liu G, Tsang S, Cai Z: **Water soluble and insoluble components of PM2.5 and their functional cardiotoxicities on neonatal rat cardiomyocytes in vitro.** *Ecotoxicol Environ Saf* 2019, **168:**378-387.
8. Calderon-Garciduenas L, Solt AC, Henriquez-Roldan C, Torres-Jardon R, Nuse B, Herritt L, Villarreal-Calderon R, Osnaya N, Stone I, Garcia R, et al: **Long-term air**

pollution exposure is associated with neuroinflammation, an altered innate immune response, disruption of the blood-brain barrier, ultrafine particulate deposition, and accumulation of amyloid beta-42 and alpha-synuclein in children and young adults. *Toxicol Pathol* 2008, **36:**289-310.

9. Calderon-Garciduenas L, Franco-Lira M, Henriquez-Roldan C, Osnaya N, Gonzalez-Maciel A, Reynoso-Robles R, Villarreal-Calderon R, Herritt L, Brooks D, Keefe S, et al: **Urban air pollution: influences on olfactory function and pathology in exposed children and young adults.** *Exp Toxicol Pathol* 2010, **62:**91-102.

10. Calderon-Garciduenas L, Gonzalez-Maciel A, Reynoso-Robles R, Kulesza RJ, Mukherjee PS, Torres-Jardon R, Ronkko T, Doty RL: **Alzheimer's disease and alpha-synuclein pathology in the olfactory bulbs of infants, children, teens and adults </=40 years in Metropolitan Mexico City. APOE4 carriers at higher risk of suicide accelerate their olfactory bulb pathology.** *Environ Res* 2018, **166:**348-362.

11. Shin S, Burnett RT, Kwong JC, Hystad P, van Donkelaar A, Brook JR, Copes R, Tu K, Goldberg MS, Villeneuve PJ, et al: **Effects of ambient air pollution on incident Parkinson's disease in Ontario, 2001 to 2013: a population-based cohort study.** *Int J Epidemiol* 2018, **47:**2038-2048.

12. Zhang T, Zheng X, Wang X, Zhao H, Wang T, Zhang H, Li W, Shen H, Yu L: **Maternal Exposure to PM2.5 during Pregnancy Induces Impaired Development of Cerebral Cortex in Mice Offspring.** *Int J Mol Sci* 2018, **19**.

13. Liu F, Huang Y, Zhang F, Chen Q, Wu B, Rui W, Zheng JC, Ding W: **Macrophages treated with particulate matter PM2.5 induce selective neurotoxicity through glutaminase-mediated glutamate generation.** *J Neurochem* 2015, **134:**315-326.

14. Chen L, Yokel RA, Hennig B, Toborek M: **Manufactured aluminum oxide**

nanoparticles decrease expression of tight junction proteins in brain vasculature. *J Neuroimmune Pharmacol* 2008, **3:**286-295.

15. Alzheimer's A: **2016 Alzheimer's disease facts and figures.** *Alzheimers Dement* 2016, **12:**459-509.

16. Canet G, Chevallier N, Zussy C, Desrumaux C, Givalois L: **Central Role of Glucocorticoid Receptors in Alzheimer's Disease and Depression.** *Front Neurosci* 2018, **12:**739.

17. Troncoso-Escudero P, Parra A, Nassif M, Vidal RL: **Outside in: Unraveling the Role of Neuroinflammation in the Progression of Parkinson's Disease.** *Front Neurol* 2018, **9:**860.

18. Akhter H, Ballinger C, Liu N, van Groen T, Postlethwait EM, Liu RM: **Cyclic Ozone Exposure Induces Gender-Dependent Neuropathology and Memory Decline in an Animal Model of Alzheimer's Disease.** *Toxicol Sci* 2015, **147:**222-234.

19. Calderon-Garciduenas L, Reed W, Maronpot RR, Henriquez-Roldan C, Delgado-Chavez R, Calderon-Garciduenas A, Dragustinovis I, Franco-Lira M, Aragon-Flores M, Solt AC, et al: **Brain inflammation and Alzheimer's-like pathology in individuals exposed to severe air pollution.** *Toxicol Pathol* 2004, **32:**650-658.

20. Kawahara M, Kato-Negishi M: **Link between Aluminum and the Pathogenesis of Alzheimer's Disease: The Integration of the Aluminum and Amyloid Cascade Hypotheses.** *Int J Alzheimers Dis* 2011, **2011:**276393.

21. Malm TM, Jay TR, Landreth GE: **The evolving biology of microglia in Alzheimer's disease.** *Neurotherapeutics* 2015, **12:**81-93.

22. Sarlus H, Heneka MT: **Microglia in Alzheimer's disease.** *J Clin Invest* 2017, **127:**3240-3249.

23. Ku T, Li B, Gao R, Zhang Y, Yan W, Ji X, Li G, Sang N: **NF-kappaB-regulated**

microRNA-574-5p underlies synaptic and cognitive impairment in response to atmospheric PM2.5 aspiration. *Part Fibre Toxicol* 2017, **14:**34.

24. Wang Z, Gerstein M, Snyder M: **RNA-Seq: a revolutionary tool for transcriptomics.** *Nat Rev Genet* 2009, **10:**57-63.

25. Su Z, Fang H, Hong H, Shi L, Zhang W, Zhang W, Zhang Y, Dong Z, Lancashire LJ, Bessarabova M, et al: **An investigation of biomarkers derived from legacy microarray data for their utility in the RNA-seq era.** *Genome Biol* 2014, **15:**523.

26. Lei X, Muscat JE, Huang Z, Chen C, Xiu G, Chen J: **Differential transcriptional changes in human alveolar epithelial A549 cells exposed to airborne PM2.5 collected from Shanghai, China.** *Environ Sci Pollut Res Int* 2018, **25:**33656-33666.

27. Saunders V, Breysse P, Clark J, Sproles A, Davila M, Wills-Karp M: **Particulate matter-induced airway hyperresponsiveness is lymphocyte dependent.** *Environ Health Perspect* 2010, **118:**640-646.

28. Lau AA, Crawley AC, Hopwood JJ, Hemsley KM: **Open field locomotor activity and anxiety-related behaviors in mucopolysaccharidosis type IIIA mice.** *Behav Brain Res* 2008, **191:**130-136.

29. Walf AA, Frye CA: **The use of the elevated plus maze as an assay of anxiety-related behavior in rodents.** *Nat Protoc* 2007, **2:**322-328.

30. Rodgers RJ, Johnson NJ: **Factor analysis of spatiotemporal and ethological measures in the murine elevated plus-maze test of anxiety.** *Pharmacol Biochem Behav* 1995, **52:**297-303.

31. Slattery DA, Cryan JF: **Modelling depression in animals: at the interface of reward and stress pathways.** *Psychopharmacology (Berl)* 2017, **234:**1451-1465.

32. Benelli A, Filaferro M, Bertolini A, Genedani S: **Influence of S-adenosyl-L-methionine on chronic mild stress-induced anhedonia in castrated rats.** *Br J*

672 *Pharmacol* 1999, **127:**645-654.
673 33. Yang C, Fang X, Zhan G, Huang N, Li S, Bi J, Jiang R, Yang L, Miao L, Zhu B, et al:
674 **Key role of gut microbiota in anhedonia-like phenotype in rodents with**
675 **neuropathic pain.** *Transl Psychiatry* 2019, **9:**57.
676 34. Li S, Yang C, Fang X, Zhan G, Huang N, Gao J, Xu H, Hashimoto K, Luo A: **Role of**
677 **Keap1-Nrf2 Signaling in Anhedonia Symptoms in a Rat Model of Chronic**
678 **Neuropathic Pain: Improvement With Sulforaphane.** *Front Pharmacol* 2018,
679 **9:**887.
680 35. Zeldetz V, Natanel D, Boyko M, Zlotnik A, Shiyntum HN, Grinshpun J, Frank D,
681 Kuts R, Brotfain E, Peiser J: **A New Method for Inducing a Depression-Like**
682 **Behavior in Rats.** *J Vis Exp* 2018.
683 36. G.M. MR: **Spatial localization does not require the presence of local cues.**
684 *Academic Press* 1981, **12**.
685 37. Gee MS, Son SH, Jeon SH, Do J, Kim N, Ju YJ, Lee SJ, Chung EK, Inn KS, Kim NJ,
686 Lee JK: **A selective p38alpha/beta MAPK inhibitor alleviates neuropathology and**
687 **cognitive impairment, and modulates microglia function in 5XFAD mouse.**
688 *Alzheimers Res Ther* 2020, **12:**45.
689 38. Ghafouri S, Fathollahi Y, Javan M, Shojaei A, Asgari A, Mirnajafi-Zadeh J: **Effect of**
690 **low frequency stimulation on impaired spontaneous alternation behavior of**
691 **kindled rats in Y-maze test.** *Epilepsy Res* 2016, **126:**37-44.
692 39. Sierksma AS, van den Hove DL, Pfau F, Philippens M, Bruno O, Fedele E, Ricciarelli
693 R, Steinbusch HW, Vanmierlo T, Prickaerts J: **Improvement of spatial memory**
694 **function in APPswe/PS1dE9 mice after chronic inhibition of phosphodiesterase**
695 **type 4D.** *Neuropharmacology* 2014, **77:**120-130.
696 40. Liu CQ, Chen Z, Liu FX, Hu DN, Luo JH: **Involvement of brain endogenous**

histamine in the degeneration of dopaminergic neurons in 6-hydroxydopamine-lesioned rats. *Neuropharmacology* 2007, **53:**832-841.

41. Liu CQ, Shan L, Balesar R, Luchetti S, Van Heerikhuize JJ, Luo JH, Swaab DF, Bao AM: **A quantitative in situ hybridization protocol for formalin-fixed paraffin-embedded archival post-mortem human brain tissue.** *Methods* 2010, **52:**359-366.

42. McGregor R, Shan L, Wu MF, Siegel JM: **Diurnal fluctuation in the number of hypocretin/orexin and histamine producing: Implication for understanding and treating neuronal loss.** *PLoS One* 2017, **12:**e0178573.

43. Zhou P, Homberg JR, Fang Q, Wang J, Li W, Meng X, Shen J, Luan Y, Liao P, Swaab DF, et al: **Histamine-4 receptor antagonist JNJ7777120 inhibits pro-inflammatory microglia and prevents the progression of Parkinson-like pathology and behaviour in a rat model.** *Brain Behav Immun* 2019, **76:**61-73.

44. Ohsawa K, Imai Y, Sasaki Y, Kohsaka S: **Microglia/macrophage-specific protein Iba1 binds to fimbrin and enhances its actin-bundling activity.** *J Neurochem* 2004, **88:**844-856.

45. Friedrich P, Aszodi A: **MAP2: a sensitive cross-linker and adjustable spacer in dendritic architecture.** *FEBS Lett* 1991, **295:**5-9.

46. Labzin LI, Heneka MT, Latz E: **Innate Immunity and Neurodegeneration.** *Annu Rev Med* 2018, **69:**437-449.

47. Yuan Y, Zha H, Rangarajan P, Ling EA, Wu C: **Anti-inflammatory effects of Edaravone and Scutellarin in activated microglia in experimentally induced ischemia injury in rats and in BV-2 microglia.** *BMC Neurosci* 2014, **15:**125.

48. Roque PJ, Dao K, Costa LG: **Microglia mediate diesel exhaust particle-induced cerebellar neuronal toxicity through neuroinflammatory mechanisms.** *Neurotoxicology* 2016, **56:**204-214.

49. Dong L, Sun W, Li F, Shi M, Meng X, Wang C, Meng M, Tang W, Liu H, Wang L, Song L: **The harmful effects of acute PM2.5 exposure to the heart and a novel preventive and therapeutic function of CEOs.** *Sci Rep* 2019, **9:**3495.

50. G O, MJ U: **Ultrafine particles in the urban air: to the respiratory tract--and beyond?** *Environmental health perspectives* 2002, **110:**A440-441.

51. Prueitt RL, Cohen JM, Goodman JE: **Evaluation of atherosclerosis as a potential mode of action for cardiovascular effects of particulate matter.** *Regul Toxicol Pharmacol* 2015, **73:**S1-15.

52. Vidrio E, Jung H, Anastasio C: **Generation of Hydroxyl Radicals from Dissolved Transition Metals in Surrogate Lung Fluid Solutions.** *Atmos Environ (1994)* 2008, **42:**4369-4379.

53. Mosmiller LT, Steele KN, Shrader CD, Petrone AB: **Evaluation of inflammatory cell biomarkers in chronic venous insufficiency.** *Phlebology* 2017, **32:**634-640.

54. Gupta P, Sil S, Ghosh R, Ghosh A, Ghosh T: **Intracerebroventricular Abeta-Induced Neuroinflammation Alters Peripheral Immune Responses in Rats.** *J Mol Neurosci* 2018, **66:**572-586.

55. Morgan TE, Davis DA, Iwata N, Tanner JA, Snyder D, Ning Z, Kam W, Hsu YT, Winkler JW, Chen JC, et al: **Glutamatergic neurons in rodent models respond to nanoscale particulate urban air pollutants in vivo and in vitro.** *Environ Health Perspect* 2011, **119:**1003-1009.

56. Modrego PJ: **Depression in Alzheimer's disease. Pathophysiology, diagnosis, and treatment.** *J Alzheimers Dis* 2010, **21:**1077-1087.

57. Kokmen E, Beard CM, Chandra V, Offord KP, Schoenberg BS, Ballard DJ: **Clinical risk factors for Alzheimer's disease: a population-based case-control study.** *Neurology* 1991, **41:**1393-1397.

58. Muzzi M, Gerace E, Buonvicino D, Coppi E, Resta F, Formentini L, Zecchi R, Tigli L, Guasti D, Ferri M, et al: **Dexpramipexole improves bioenergetics and outcome in experimental stroke.** *Br J Pharmacol* 2018, **175:**272-283.

59. Pereira JB, Svenningsson P, Weintraub D, Bronnick K, Lebedev A, Westman E, Aarsland D: **Initial cognitive decline is associated with cortical thinning in early Parkinson disease.** *Neurology* 2014, **82:**2017-2025.

60. Scarr E, McLean C, Dean B: **Higher levels of different muscarinic receptors in the cortex and hippocampus from subjects with Alzheimer's disease.** *J Neural Transm (Vienna)* 2017, **124:**273-284.

61. Cheng L, Lau WKW, Fung TKH, Lau BWM, Chau BKH, Liang Y, Wang Z, So KF, Wang T, Chan CCH, Lee TMC: **PM2.5 Exposure Suppresses Dendritic Maturation in Subgranular Zone in Aged Rats.** *Neurotox Res* 2017, **32:**50-57.

62. Luk KC, Kehm V, Carroll J, Zhang B, O'Brien P, Trojanowski JQ, Lee VM: **Pathological alpha-synuclein transmission initiates Parkinson-like neurodegeneration in nontransgenic mice.** *Science* 2012, **338:**949-953.

63. Li Y, Tan MS, Jiang T, Tan L: **Microglia in Alzheimer's disease.** *Biomed Res Int* 2014, **2014:**437483.

Figure 1. The systemic inflammation of mice after long term $PM_{2.5}$ exposure.

Flow cytometric analysis showed that $PM_{2.5}$ increased the percentage of CD11b+ splenocytes in the young, old and the APP/PS transgenic AD groups. The results are expressed as the mean ± SEM (6 mice/group) **P<0.01; ***P<0.001 vs Control group.

Figure 2. The spatial learning and memory of mice after long term $PM_{2.5}$ exposure.

A) The escape latency to the hidden platform during days 2–5 of training; B) Escape latency on the fifth day; C) Swimming speed on the fifth day; D) Percentage of time spent in the target quadrant. E) Number of times crossing the target quadrant; F) Percentage of swimming distance in the target quadrant; G) Percentage of spontaneous alternation behavior; H) Number of total arm entries. Data are present as the mean ± SEM (6 mice/group). *P<0.05; **P<0.01;***P<0.001 vs Control group.

Figure 3. The affective behaviors changes after long term $PM_{2.5}$ exposure.

A) The body weight of mice; B) The time spent in open arms; C) The percentage of sucrose consumption. The results are expressed as the mean ± SEM (6 mice/group). *P<0.05; ***P<0.001 vs Control group.

Figure 4. Hippocampal and cortex neuron damage visualized by Nissl staining.

A) The representative images of Nissl stained the hippocampal CA1 area of control group and $PM_{2.5}$ treatment group (40×). B) The representative images of Nissl stained the cortex area of control groups and $PM_{2.5}$ treatment groups (40×). The results are expressed as the mean ± SEM (6 mice/group). **P<0.01 vs Control group. $^{\#}$P<0.05; $^{\#\#}$P<0.01 vs Young groups after $PM_{2.5}$ exposure.

Figure 5. Immunohistochemical staining for MAP2 in the hippocampus after long term $PM_{2.5}$ exposure.

The representative immunohistochemical staining image for MAP2 in hippocampus CA1 area (40×). The results are expressed as the mean ± SEM (6 mice/group).**P<0.01; ***P<0.001 vs Control group. $^{\#\#}$P<0.01; $^{\#\#\#}$P<0.001 vs Young groups after $PM_{2.5}$ exposure.

Figure 6. Immunohistochemical staining for Aβ1-42 in hippocampus after long term $PM_{2.5}$ exposure.

The representative immunohistochemical staining image for Aβ1-42 in hippocampus CA1 area (20×). The results are expressed as the mean ± SEM (6 mice/group). ***P<0.001 vs Control group; $^{\#\#\#}$P<0.001 vs Young groups after $PM_{2.5}$ exposure.

Figure 7. Analysis of differentially expressed genes between control and $PM_{2.5}$ groups.

A) Gene expression level of control versus $PM_{2.5}$ groups. P<0.05 were used as the threshold to judge the significance of gene expression difference. B) The heat map and hierarchical clustering of differentially expressed mRNAs between control and $PM_{2.5}$ groups (3 mice/group).

Figure8. Gene Ontology (GO) classification of genes differentially expressed between control and $PM_{2.5}$ groups.

The functions of genes identified cover three main categories: biological process, cellular component, and molecular function. Bars represent −log10 (*p* value).

Figure9. KEGG pathways analysis of genes differentially expressed between control and $PM_{2.5}$ groups.

822 The significant pathways for the different expression genes. Bars represent −log10 (*p* value).

823

824 **Figure10. Microglia related gene and protein changes after $PM_{2.5}$ exposure.**

825 $PM_{2.5}$ exposure increased the mRNA expression of M1 microglia marker CD86(A) and the

826 expression of CD22(D) and IL-1β(E). $PM_{2.5}$ exposure decreased the expression of M2

827 microglia marker CD206(B) and the expression of TREM2(C) and TGF-b2(F).

828 Representative immunohistochemical staining image for IBA-1 positive cells in hippocampus

829 CA1 area (40×) (G, H). The results are expressed as the mean ± SEM (6 mice/group).

830 *P<0.05; **P<0.01 vs Control group. $^{\#}$P<0.05; $^{\#\#\#}$P<0.001 vs Young groups after $PM_{2.5}$

831 exposure.

Figures

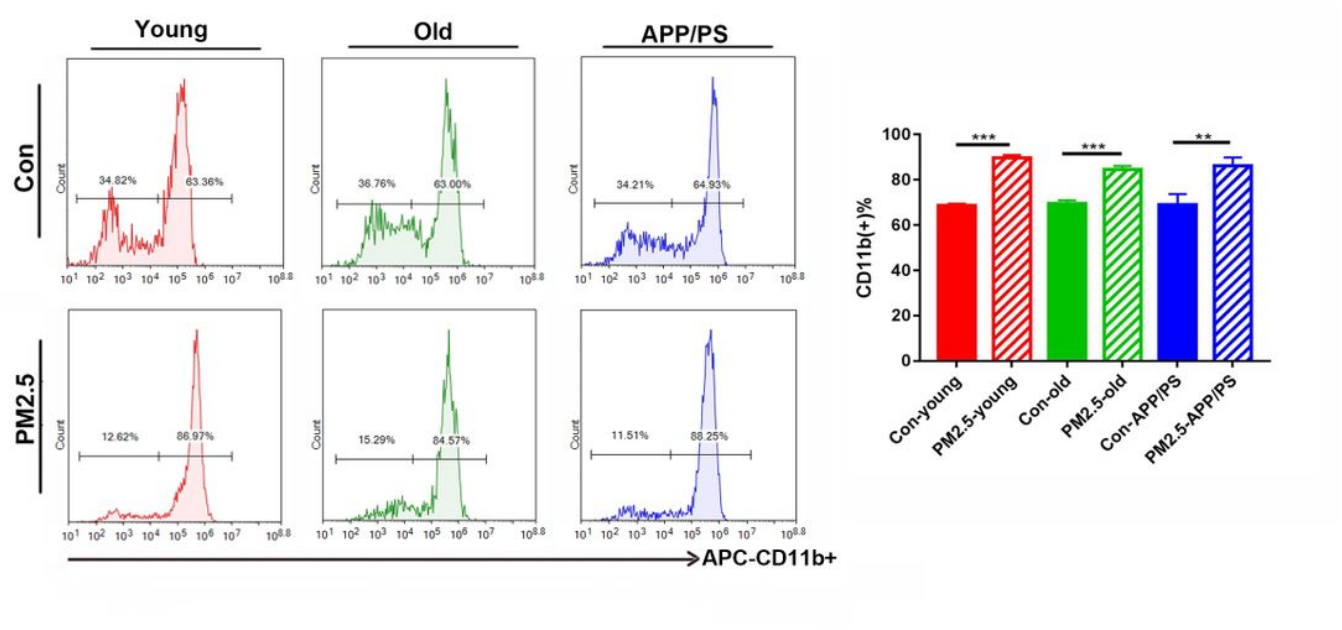

Figure 1

The systemic inflammation of mice after long term PM2.5 exposure. Flow cytometric analysis showed that PM2.5 increased the percentage of CD11b+ splenocytes in the young, old and the APP/PS transgenic AD groups. The results are expressed as the mean ± SEM (6 mice/group) **P<0.01; ***P<0.001 vs Control group.

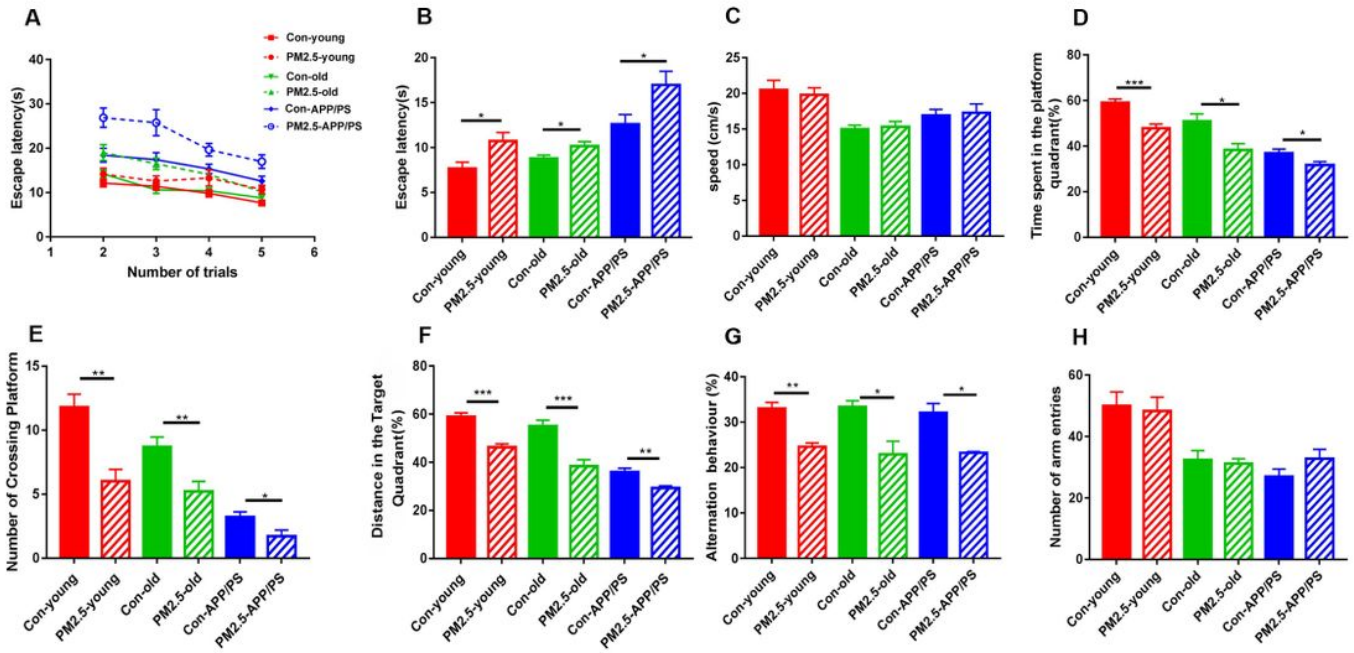

Figure 2

The spatial learning and memory of mice after long term PM2.5 exposure. A) The escape latency to the hidden platform during days 2–5 of training; B) Escape latency on the fifth day; C) Swimming speed on the fifth day; D) Percentage of time spent in the target quadrant. E) Number of times crossing the target quadrant; F) Percentage of swimming distance in the target quadrant; G) Percentage of spontaneous alternation behavior; H) Number of total arm entries. Data are present as the mean ± SEM (6 mice/group). *P<0.05; **P<0.01;***P<0.001 vs Control group.

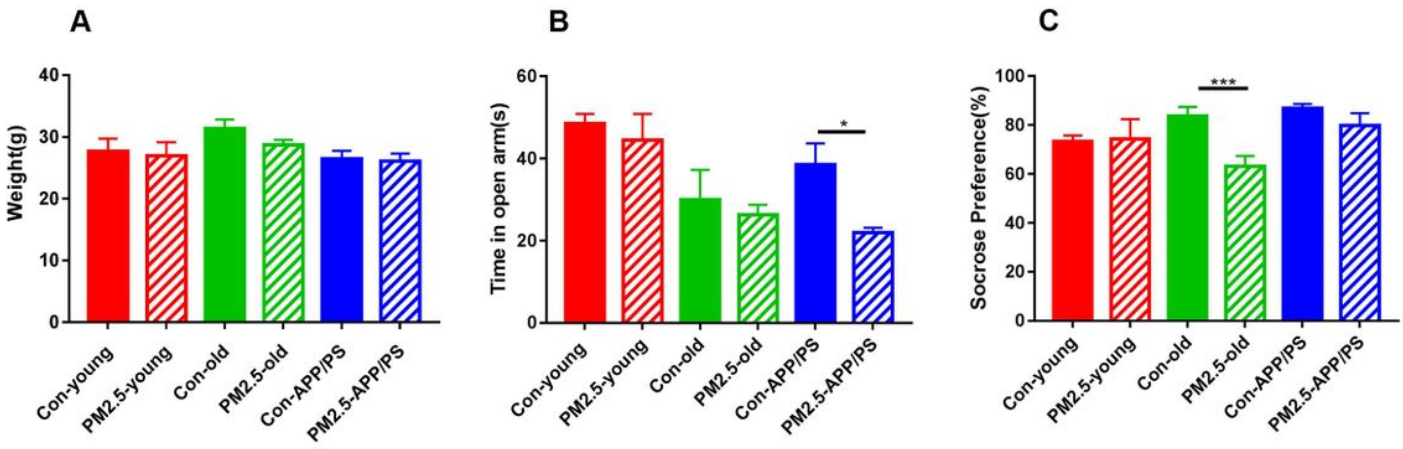

Figure 3

The affective behaviors changes after long term PM2.5 exposure. A) The body weight of mice; B) The time spent in open arms; C) The percentage of sucrose consumption. The results are expressed as the mean ± SEM (6 mice/group). *P<0.05; ***P<0.001 vs Control group.

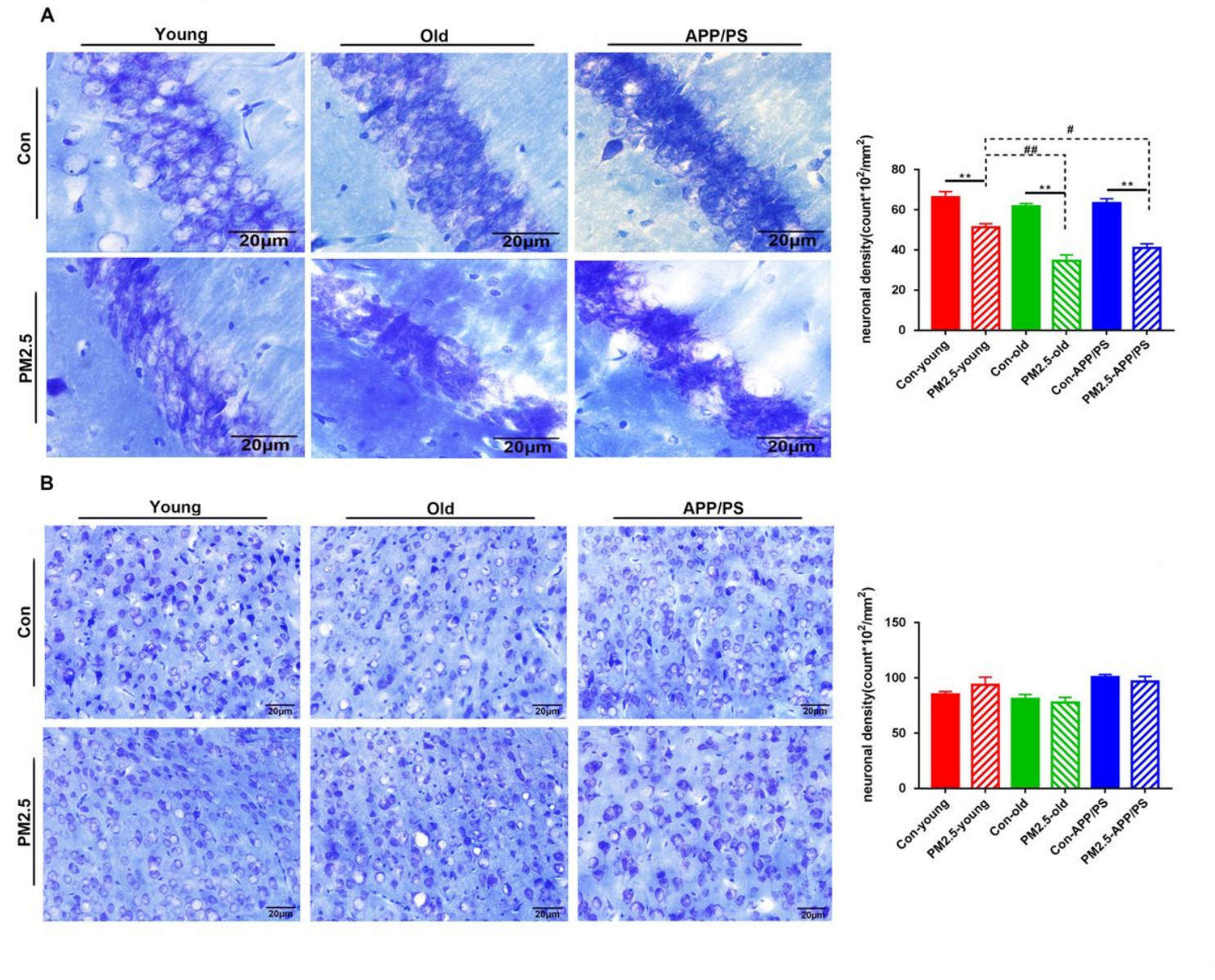

Figure 4

Hippocampal and cortex neuron damage visualized by Nissl staining. A) The representative images of Nissl stained the hippocampal CA1 area of control group and PM2.5 treatment group (40×). B) The representative images of Nissl stained the cortex area of control groups and PM2.5 treatment groups (40×). The results are expressed as the mean ± SEM (6 mice/group). **P<0.01 vs Control group. #P<0.05; ##P<0.01 vs Young groups after PM2.5 exposure.

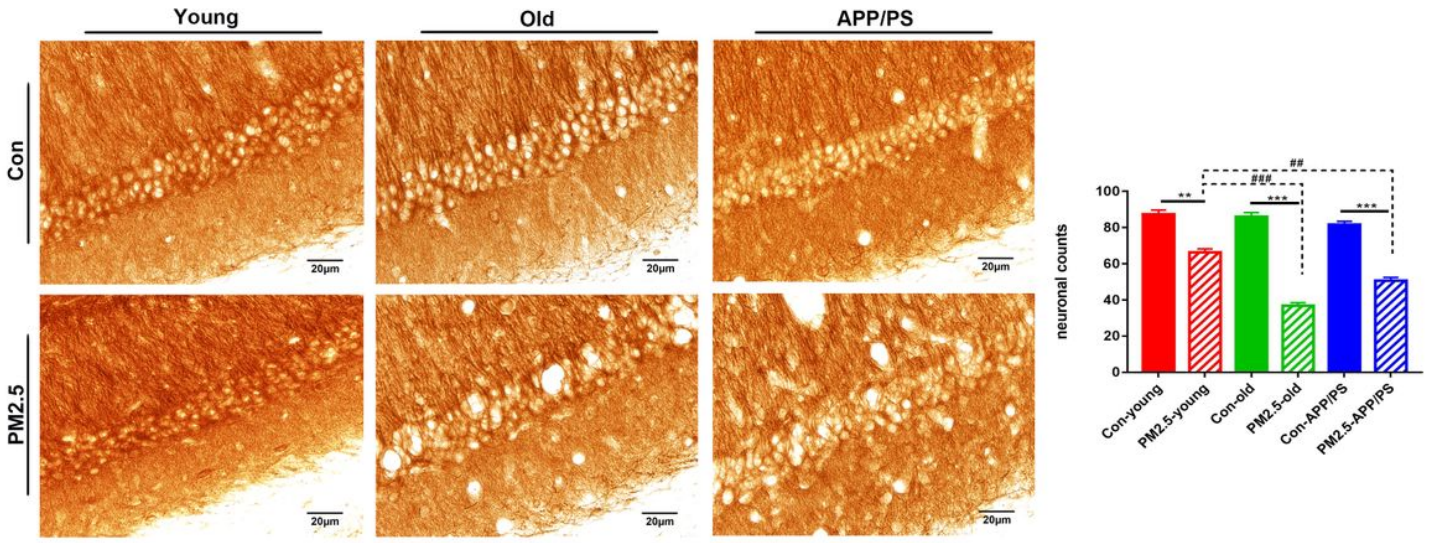

Figure 5

Immunohistochemical staining for MAP2 in the hippocampus after long term PM2.5 exposure. The representative immunohistochemical staining image for MAP2 in hippocampus CA1 area (40×). The results are expressed as the mean ± SEM (6 mice/group).**P<0.01; ***P<0.001 vs Control group. ##P<0.01; ###P<0.001 vs Young groups after PM2.5 exposure.

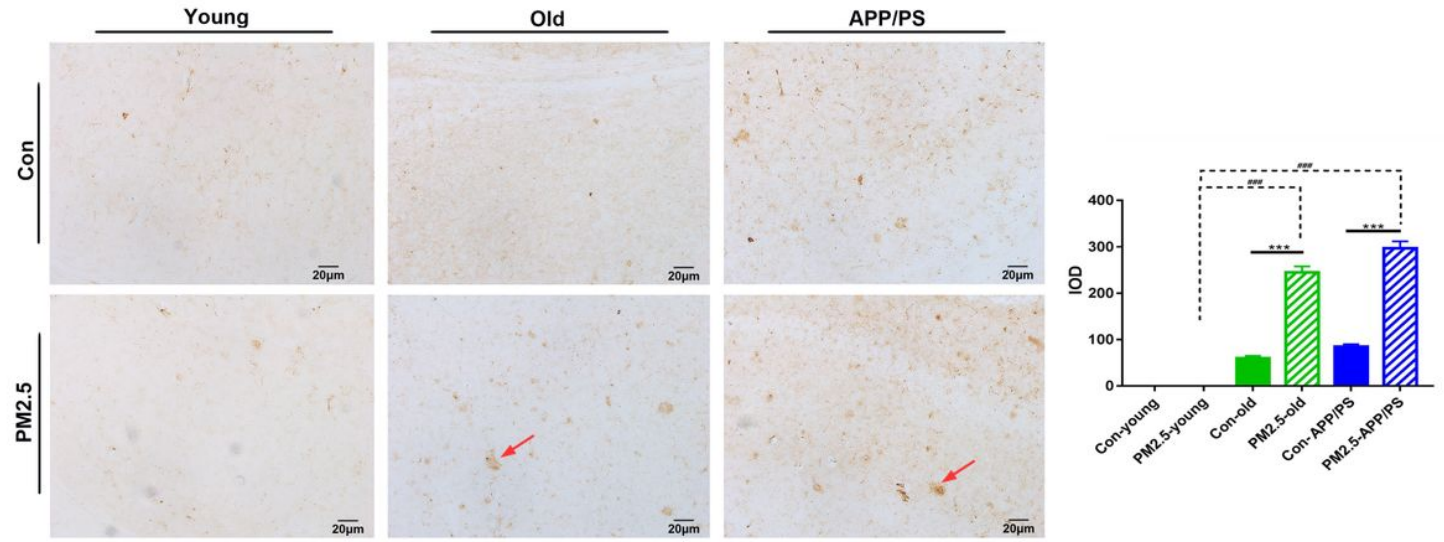

Figure 6

Immunohistochemical staining for Aβ1-42 in hippocampus after long term PM2.5 exposure. The representative immunohistochemical staining image for Aβ1-42 in hippocampus CA1 area (20×). The results are expressed as the mean ± SEM (6 mice/group). ***P<0.001 vs Control group; ###P<0.001 vs Young groups after PM2.5 exposure.

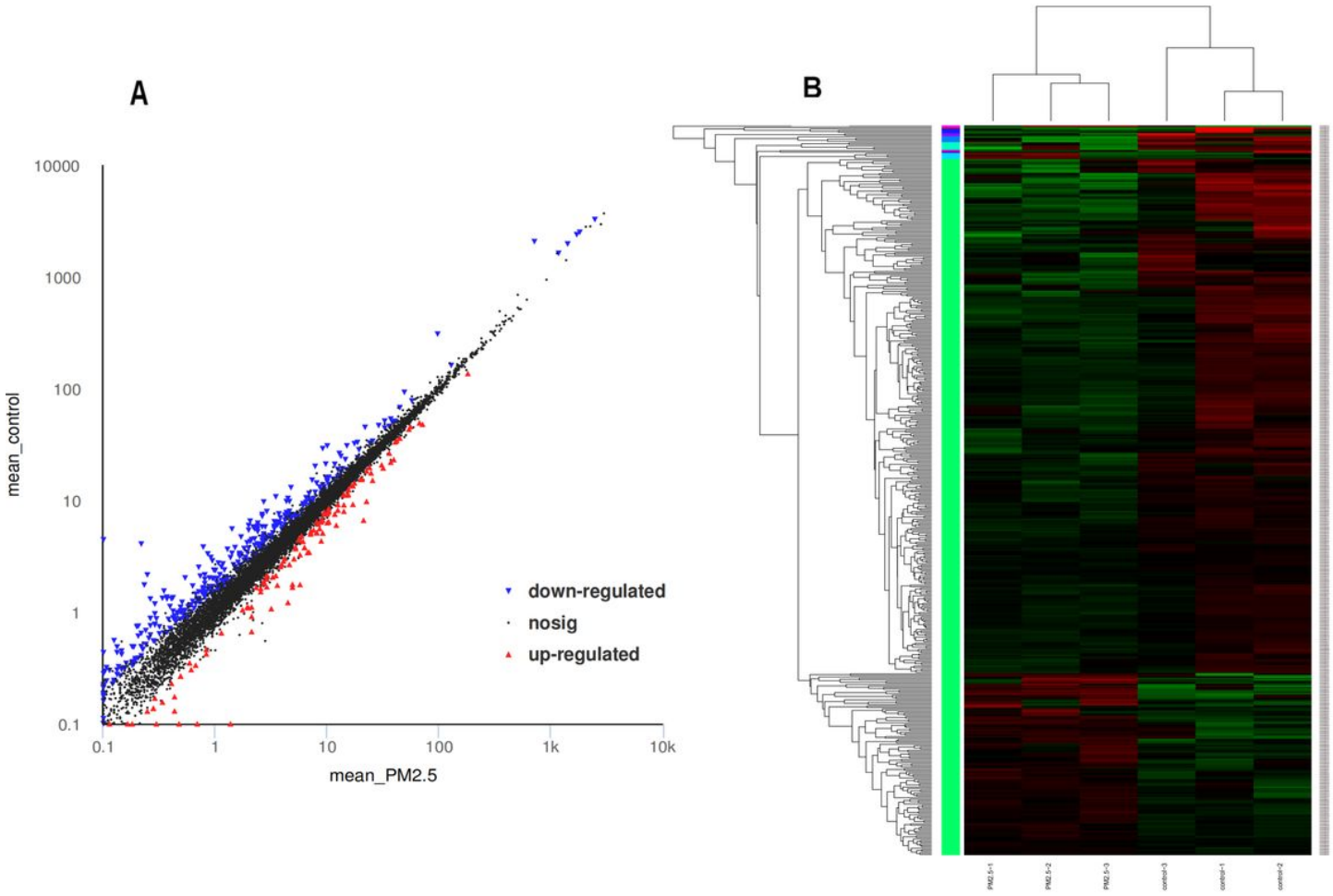

Figure 7

Analysis of differentially expressed genes between control and PM2.5 groups. A) Gene expression level of control versus PM2.5 groups. P<0.05 were used as the threshold to judge the significance of gene expression difference. B) The heat map and hierarchical clustering of differentially expressed mRNAs between control and PM2.5 groups (3 mice/group).

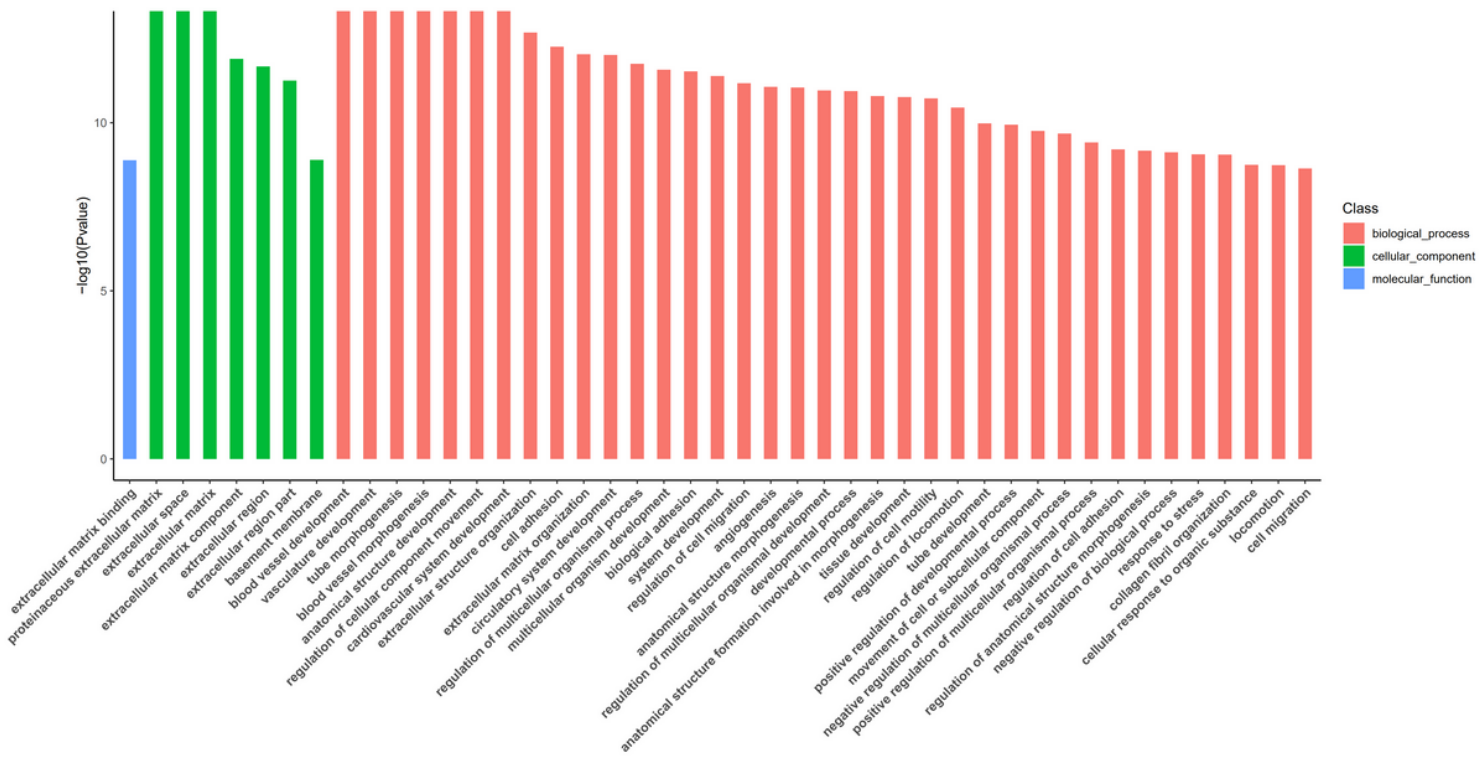

Figure 8

Gene Ontology (GO) classification of genes differentially expressed between control and PM2.5 groups. The functions of genes identified cover three main categories: biological process, cellular component, and molecular function. Bars represent −log10 (p value).

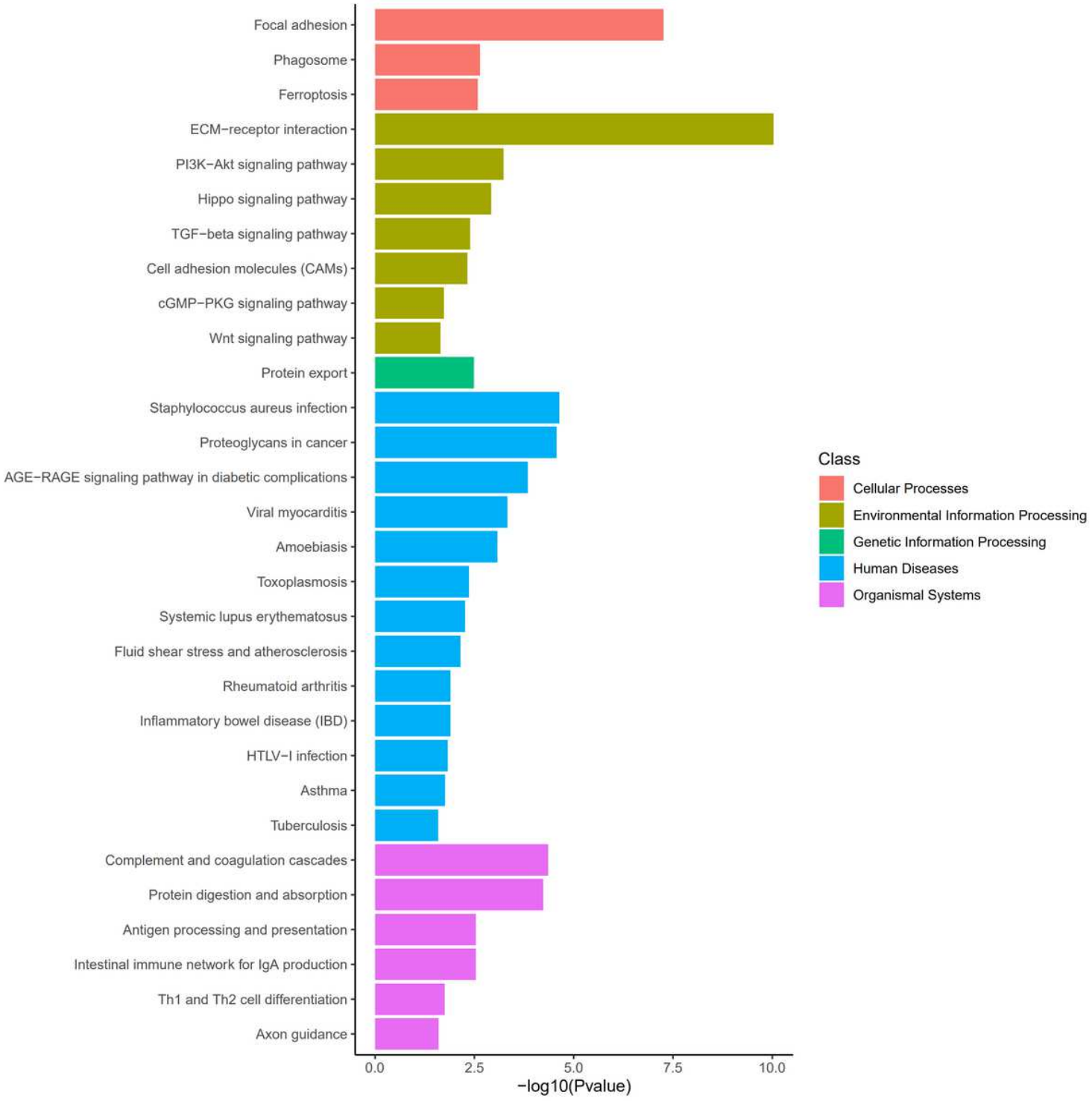

Figure 9

KEGG pathways analysis of genes differentially expressed between control and PM2.5 groups. The significant pathways for the different expression genes. Bars represent −log10 (p value).

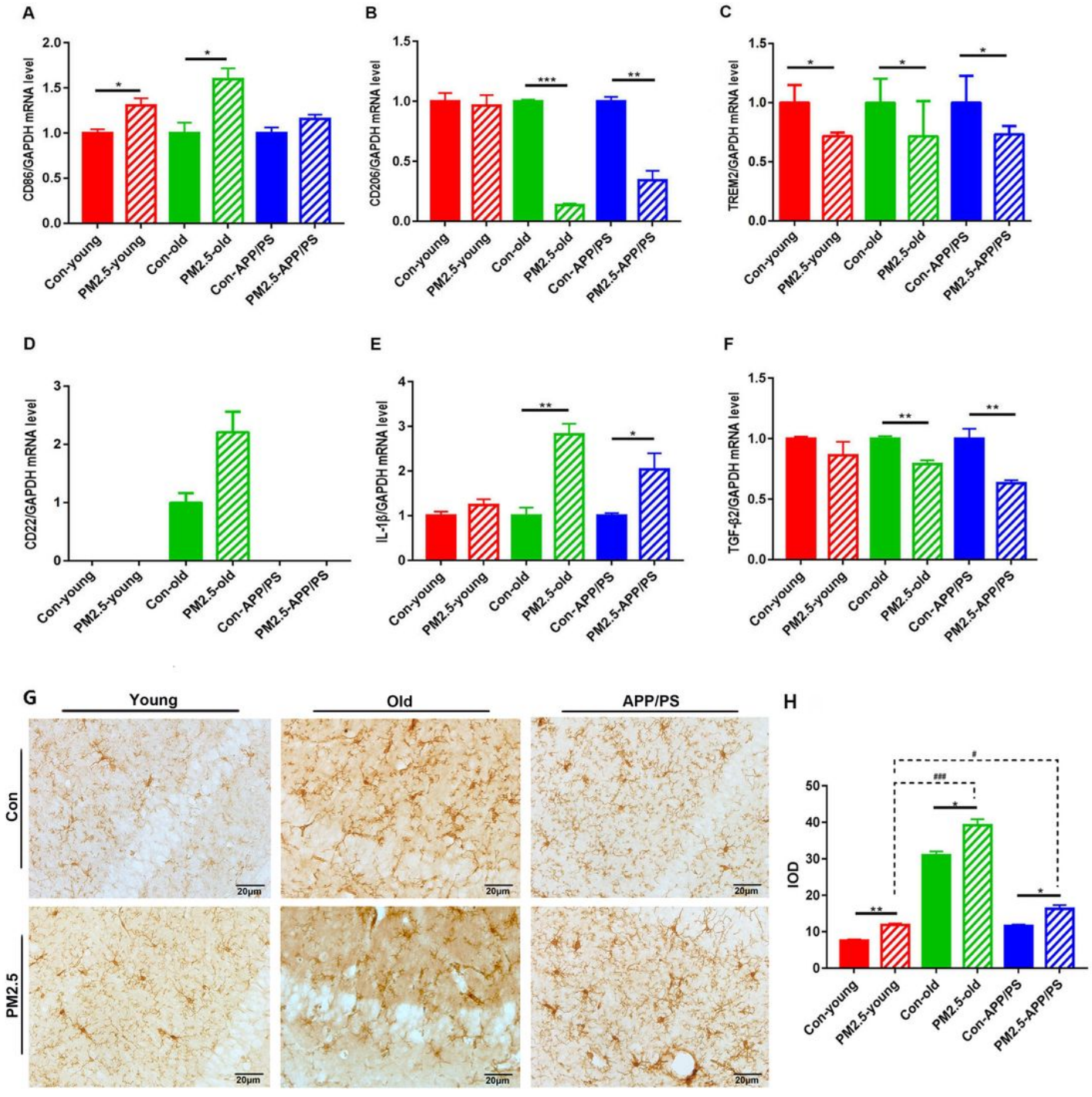

Figure 10

Microglia related gene and protein changes after PM2.5 exposure. PM2.5 exposure increased the mRNA expression of M1 microglia marker CD86(A) and the expression of CD22(D) and IL-1β(E). PM2.5 exposure decreased the expression of M2 microglia marker CD206(B) and the expression of TREM2(C) and TGF-b2(F). Representative immunohistochemical staining image for IBA-1 positive cells in hippocampus CA1

area (40×) (G, H). The results are expressed as the mean ± SEM (6 mice/group). *P<0.05; **P<0.01 vs Control group. #P<0.05; ###P<0.001 vs Young groups after PM2.5 exposure.